Communicated by Kenneth Miller

Understanding Retinal Color Coding from First Principles

Joseph J. Atick
Zhaoping Li
A. Norman Redlich
School of Natural Sciences, Institute for Advanced Study, Princeton, NJ 08540 USA

A previously proposed theory of visual processing, based on redundancy reduction, is used to derive the retinal transfer function including color. The predicted kernels show the nontrivial mixing of space–time with color coding observed in experiments. The differences in color coding between species are found to be due to differences among the chromatic autocorrelators for natural scenes in different environments.

1 Introduction

The retinas of many species code color signals in a nontrivial way that is strongly coupled to their coding of spatial and temporal information. For example, in the primate retina many color coding ganglion cells are excited by "green" light[1] falling on the centers of their *receptive fields* on the retina, but their response is inhibited by "red" light falling in a concentric annulus about the green center — called the surround region of their receptive field. There are also red center, green surround cells (Derrington *et al.* 1984) as well as rarer types involving blue cones. Such arrangements, which can be termed "single-opponency," are not the only types found in nature. For example, freshwater fish such as goldfish and carp have a different type of coding called "double-opponency" (Daw 1968). Their ganglion cells are color opponent — they calculate the difference between the outputs of different cone types at each spatial location — and they are spatially opponent (with a center surround receptive field) but their color and spatial encoding are mostly decoupled. One of the challenges for a theory of retinal processing is to account for the difference between this double-opponent goldfish code and the single-opponent primate code, as well as the range of intermediate response types observed in other species.

[1]In this paper, we use "green" and "red" to denote light with spectral frequencies exciting primarily the cones with medium and long spectral sensitivities, respectively.

In this paper, we demonstrate that the computable theory of early visual processing reported by Atick and Redlich (1990, 1992 henceforth references *I* and *II*) can explain this variety of retinal processing types. As explained at length there, the theory hypothesizes that the purpose of retinal coding is to reduce both redundancy and noise in the visual image. The idea of redundancy reduction as an efficiency goal in the sensory system was first proposed by Attneave (1954) and Barlow (1961). In the retina, redundancy in space, time, and color comes from the fact that the pixel by pixel representation of natural scenes, which is the representation formed by the photoreceptors, contains a high degree of correlations among pixels. Therefore, many pixels redundantly represent the same information. Actually with color, there is an additional source of correlation between the photoreceptor outputs coming from the overlapping spectral domains of the three cone types.

To improve efficiency, the retina can recode the photoreceptor signal to eliminate correlations in space, time, and color. In refs. *I* and *II*, it was assumed that the retina, being only the first stage in the visual pathway, can eliminate only the simplest form of redundancy, which comes from pixel–pixel correlations: second-order correlation. It makes sense for the retina to eliminate second-order correlation since it is the source of the largest fraction of redundancy in the image, and it can be eliminated relatively easily through a linear transformation that decorrelates the input (photoreceptor) signal. As shown in *I* and *II*, decorrelation together with noise reduction does give a retinal transfer function that agrees with available data from contrast sensitivity experiments. Here we take that analysis one step further and solve for the system that decorrelates at the two point level both in space and color.

What we find is that the differences seen in the color coding of primates and fish can be attributed to plausible differences in the color correlation matrix for the two species. More precisely, we note that the degree of overlap between the *R* and *G* cones in primates is greater than the corresponding overlap in fish (the *R* and *G* spectral sensitivity peaks are separated by only 32 nm for the primates but by 90 nm for the fish). This difference in photoreceptor sampling is well known to be attributed to differences between the primate visual environment and the environment under water (Lythgoe 1979). What we show in this paper is that this sampling difference has very pronounced effects on the subsequent neural processing needed to achieve decorrelation. In fact it will enable us to account for single vs. double opponency coding. In passing, we should mention that we limit our analysis to the two cone (*R* and *G*) system, since in primate retina these photoreceptors occur with equal density and are more abundant than the blue cones. In fact the blue cones constitute only 15% of the total cone population in the entire retina while in the fovea they are virtually nonexistent. We also confine ourselves to color coding by linear cells, which implies cells in the primate parvocellular pathway.

It is important to point out, however, that the mixing between space, time, and color that we derive here does not come only from decorrelation. In fact, we use here a correlation matrix which itself does *not* mix space–time with color, though such mixing in the correlation matrix can easily be included in our analysis and it only accentuates the effect found here – for the more general analysis (see Atick *et al.* 1990). It is actually noise filtering, together with redundancy reduction, which produces the nontrivial interactions. Noise filtering is a prerequisite for achieving single opponency, and it also explains the observed differences between psychophysical contrast sensitivity measurements in the luminance and chromatic channels.

We should point out that the earliest attempt to explain color opponency using decorrelation was made by Buchsbaum and Gottschalk (1983), also inspired by Barlow (1961). However, their work did not include the spatiotemporal dimensions, nor did it include noise, so it does not account for the observed nontrivial coupling of space–time and color.

2 Decorrelation and Color Coding

As in refs. *I* and *II*, we make the hypothesis that the purpose of retinal processing is to produce a more efficient representation of the incoming information by reducing redundancy. With the assumption of linear processing, the retina can eliminate only the simplest form of redundancy, namely second-order correlations. However, second-order decorrelation cannot be the only goal of retinal processing, since in the presence of noise as was argued in *II* decorrelation alone would be a dangerous computational strategy. This is due to the fact that after decorrelation both useful signal and noise are coded in a way that makes their distinction no longer possible (they both have the properties of random noise). Thus for decorrelation, or more generally redundancy reduction, to be a viable computational strategy, there must be a guarantee that no significant input noise be allowed to pass. The way we handle this noise here is similar to the approach in *II* for the purely spatial domain: we first lowpass filter to diminish noise and then decorrelate as if no noise existed.

Figure 1 is a schematic of the processing stages we assume take place in the retina. We should emphasize that this is meant to be an effective computational model and is not necessarily a model of anatomically distinct stages in the retina. As shown in the figure, the intensity signal $L(\mathbf{x}, t, \lambda)$, depending on space, time, and spectral wavelength λ, is first transduced by the photoreceptors to produce a discrete set of photoreceptor outputs,

$$P^a(\mathbf{x}, t) = \int d\lambda C^a(\lambda) L(\mathbf{x}, t, \lambda) \tag{2.1}$$

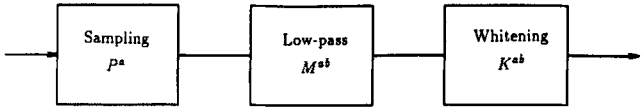

Figure 1: Schematic of the signal processing stages for the model of the retina used here. At the first stage, images are sampled by the photoreceptors to produce the chromatic signals, P^a. These are subsequently lowpass filtered by M^{ab} to eliminate noise, and then decorrelated to reduce redundancy by K^{ab}.

The functions $C^a(\lambda)$ are the spectral sensitivities of the two (more generally three) photoreceptor types, $a = 1, 2$ for R, G, respectively. Following transduction, the photoreceptor signals are lowpass filtered by a function $M^{ab}(\mathbf{x}, t; \mathbf{x}', t')$ to reduce noise. Having filtered out the noise, the final stage in Figure 1 is to reduce the redundancy using the transfer function $K^{ab}(\mathbf{x}, t; \mathbf{x}', t')$ that produces decorrelated retinal outputs. Thus the output $\mathbf{O}$ is related to the input $\mathbf{P}$ through

$$\mathbf{O} = \mathbf{K} \cdot (\mathbf{M} \cdot (\mathbf{P} + \mathbf{n}) + \mathbf{n}_0) \tag{2.2}$$

where $n^a(\mathbf{x}, t)$ is input noise including transduction and quantum noise, while $n_0(\mathbf{x}, t)$ is noise (e.g., synaptic), which is added following the filter $\mathbf{M}$. Such post-filter noise, though it may be small, must be included because it is very significant from an information theoretic point of view: it sets the scale (accuracy) for measuring the signal at the output of the filter $\mathbf{M}$. We have introduced boldface to denote matrices in the 2×2 color space; also in equation 2.2 each $\cdot$ denotes a space–time convolution.

To derive both filters $\mathbf{M}$ and $\mathbf{K}$, we require some knowledge of the statistical properties of the luminance signals $L(\mathbf{x}, t, \lambda)$: the statistical properties of natural scenes. For our linear analysis here, we only need the chromatic-spatiotemporal autocorrelator, which is a matrix of the form

$$\begin{aligned} R^{ab}(\mathbf{x}, t; \mathbf{x}', t') &= \left\langle P^a(\mathbf{x}, t) P^b(\mathbf{x}, t) \right\rangle \\ &= \int d\lambda d\lambda' C^a(\lambda) C^b(\lambda') \left\langle L(\mathbf{x}, t, \lambda) L(\mathbf{x}', t', \lambda') \right\rangle \end{aligned}$$

where $\langle\ \rangle$ denotes ensemble average. Unfortunately, not much is known experimentally about the entries of the matrix $R^{ab}(\mathbf{x}, t; \mathbf{x}', t')$. Thus, to gain insight into the color coding problem we are forced to make some assumptions. First, we assume translation invariance in space and time: $\mathbf{R}$ is then only a function of $\mathbf{x} - \mathbf{x}'$, and $t - t'$, so it can be Fourier transformed to $R^{ab}(\underline{f}, w)$, where $\underline{f}$ and w are spatial and temporal frequency,

respectively. Second, we assume $R^{ab}(\underline{f}, w)$ can be factorized into a pure spatiotemporal correlator times a 2×2 matrix describing the degree of overlap between the R and G systems. This second assumption is not absolutely necessary, since it is possible to perform the analysis entirely for the most general form of $R^{ab}(\underline{f}, w)$ (see Atick *et al.* 1990). However, this assumption does make it much simpler to analyze and explain our theoretical results. We also examine color coding only under conditions of slow temporal stimulation or near zero temporal frequency. In that case, we do have available Field's (1987) experimental measurement of the spatiotemporal correlator: $R(\underline{f}, 0) = I_0^2/|\underline{f}|^2$ with I_0 the mean background luminance of the input signal. Using this $R(\underline{f})$, and making the further simplification that the mean squared R and G photoreceptor outputs are roughly equal, we arrive at

$$\mathbf{R}(\underline{f}, 0) = \frac{I_0^2}{|\underline{f}|^2} \begin{pmatrix} 1 & r \\ r & 1 \end{pmatrix} \tag{2.3}$$

where $r < 1$ is a parameter describing the amount of overlap of R and G. We should emphasize, that we do not advocate this simple form of R^{ab} as necessarily the one found in nature. More complex R^{ab} can similarly be dealt with but they produce qualitatively similar solutions.

The next step is to use this autocorrelator to derive a noise filter $M^{ab}(\underline{f})$ (from now on we drop explicit w dependence). In ref. *II*, the principle used to derive $M(\underline{f})$, without color, was to maximize the mutual information between the output of the filter and the ideal input signal [the signal $L(\underline{f}, w)$ without noise], while constraining the total entropy of the output signal. The resulting lowpass filter cannot be complete, however, since it does not include the effects of the optics, but these can be incorporated by multiplying by the optical modulation transfer function (MTF). As discussed in detail in ref. *II*, in the absence of color (one channel problem), this gives

$$M = \frac{1}{N}\left[\frac{1}{I_0}\frac{R(\underline{f})}{R(\underline{f}) + N^2}\right]^{1/2} \exp -(|\underline{f}|/f_c)^{\alpha} \tag{2.4}$$

with N^2 the input noise power. Here, the exponential term approximates the optical MTF, which has been independently measured (Campbell and Gubisch 1966); we use typical values for the parameters α and f_c. Although, as shown in ref. *II*, this filter matches the spatial experimental data well, other filters can also give good results. For example, one may use a maximum log likelihood principle, equivalent in our case to using mean squared estimation. The really important property all such filters must have, however, is that their shape must depend on the signal to noise (S/N) at their input.

To see how color correlations (two channel problem) affect the spatiotemporal lowpass filtering, it is helpful to rotate in color space to the

basis where the color matrix is diagonal. For the simple color matrix in equation 2.3, this is a 45° rotation by

$$\mathbf{U}_{45} = \frac{1}{\sqrt{2}} \begin{pmatrix} 1 & 1 \\ -1 & 1 \end{pmatrix}$$

to the luminance, $\mathbf{G} + \mathbf{R}$, and chromatic, $\mathbf{G} - \mathbf{R}$, channels [in vector notation, the red and green channels are denoted by $\mathbf{R} = (\mathbf{1}, \mathbf{0})$ and $\mathbf{G} = (\mathbf{0}, \mathbf{1})$]. In this $\mathbf{G} \pm \mathbf{R}$ basis, the total correlation matrix, equation 2.3, plus the contribution due to noise is

$$\mathbf{U}_{45} \left(\mathbf{R}(\underline{\mathbf{f}}) + \mathbf{N}^2 \right) \mathbf{U}_{45}^T = \frac{I_0^2}{|\underline{\mathbf{f}}|^2} \begin{pmatrix} 1+r & 0 \\ 0 & 1-r \end{pmatrix} + N^2 \begin{pmatrix} 1 & 0 \\ 0 & 1 \end{pmatrix} \tag{2.5}$$

where the noise, $\langle n^a n^b \rangle = \delta^{ab} N^2$, is assumed equal in both the $\mathbf{R}$ and $\mathbf{G}$ channels, for simplicity. In the $\mathbf{G} \pm \mathbf{R}$ basis, the two color channels are decoupled. Thus, the corresponding spatiotemporal filters $M_\pm(\underline{\mathbf{f}})$ are found by applying our single-channel results, equation 2.4, independently to each channel. The $R(\underline{\mathbf{f}})$ appropriate to each $\mathbf{G} \pm \mathbf{R}$ channel is from equation 2.5,

$$R_\pm(\underline{\mathbf{f}}) = (1 \pm r) I_0^2 / |\underline{\mathbf{f}}|^2 \tag{2.6}$$

Notice that the two channels differ only in their effective S/N ratios:

$$(S/N)_\pm = \sqrt{(1 \pm r)} (I_0/N)$$

which depend multiplicatively on the color eigenvalues $1 \pm r$. In the luminance channel, $\mathbf{G} + \mathbf{R}$, the signal to noise is increased above that in either the $\mathbf{R}$ or $\mathbf{G}$ channel alone, due to the summation over the $\mathbf{R}$ and $\mathbf{G}$ signals. The filter $M_+(\underline{\mathbf{f}})$, therefore, passes relatively higher spatial and temporal frequencies, increasing spatiotemporal resolution, than without the $\mathbf{R}$ plus $\mathbf{G}$ summation. On the other hand, the chromatic channel, $\mathbf{G} - \mathbf{R}$, has lower S/N, proportional to $1 - r$, so its spatiotemporal filter $M_-(\underline{\mathbf{f}})$ cuts out higher spatial and temporal frequencies, thus sacrificing spatiotemporal resolution in favor of color discriminability. The complete filter in the original basis is finally obtained by rotating from the diagonal basis back by 45°

$$M^{ab}(\underline{\mathbf{f}}) = \frac{1}{2} \begin{pmatrix} 1 & -1 \\ 1 & 1 \end{pmatrix} \begin{pmatrix} M_+(\underline{\mathbf{f}}) & 0 \\ 0 & M_-(\underline{\mathbf{f}}) \end{pmatrix} \begin{pmatrix} 1 & 1 \\ -1 & 1 \end{pmatrix}$$

[Again $M_\pm(\underline{\mathbf{f}})$ is given by equation 2.4 with $R(\underline{\mathbf{f}}) \to R_\pm(\underline{\mathbf{f}})$ in equation 2.6.]

After filtering noise, the next step is to reduce redundancy using the transfer function $K^{ab}(\underline{\mathbf{f}}, w)$.[2] At the photoreceptor level, most of the

[2]By redundancy here, as in ref. *II*, we mean the difference between the average information H calculated using the joint probabilities for the neural outputs, and the sum of the "bit" entropies $\sum_i H_i$, calculated treating the ith neuron completely inde-

redundancy is due to second-order statistics: autocorrelation. If we ignore noise for the moment, then this redundancy can be eliminated, as shown in ref. *II*, by a linear transformation $K^{ab}(\mathbf{x} - \mathbf{x}')$ that diagonalizes the correlation matrix $R^{ab}(\mathbf{x} - \mathbf{x}')$ so that at second-order the signals are statistically independent: $\mathbf{K} \cdot \mathbf{R} \cdot \mathbf{K}^T = \mathbf{D}$ with $\mathbf{D}$ a diagonal matrix both in color and space–time. This, does not, however, uniquely specify $\mathbf{K}$ since the matrix $\mathbf{D}$ is still an arbitrary diagonal matrix. In the spatiotemporal case, we found a unique solution by requiring a translationally invariant, local set of retinal filters: the approximation where all retinal ganglion cells (in some local neighborhood, at least) have the same receptive fields, except translated on the retina, and these fields sum from only a nearby set of photoreceptor inputs. These assumptions force $\mathbf{D}$ to be proportional to the unit matrix: $\mathbf{D} = \rho\mathbf{1}$, with proportionality constant ρ. This gives in frequency space, the *whitening* filter

$$K(\underline{\mathbf{f}}) = \sqrt{\rho / R(\underline{\mathbf{f}})}$$

In generalizing this to include color, we note that when D is proportional to the unit matrix, the mean squared outputs $[(KRK^T)^{aa}_{xx}$ for output $O^a_x]$ of all ganglion cells are equal. This equalization provides efficient use of optic nerve cables (ganglion cell axons) if the set of cables for the cells in a local neighborhood has similar information-carrying capacity. We therefore continue to take $\mathbf{D}$ proportional to the identity matrix in the combined space–time–color system.

Taking $\mathbf{D}$ proportional to the identity, however, leaves a symmetry, since one can still rotate by a 2×2 orthogonal matrix U^{ab}_θ, that is, $\mathbf{K}(\underline{\mathbf{f}}) \rightarrow \mathbf{U}_\theta \mathbf{K}(\underline{\mathbf{f}})$, which leaves $\mathbf{D}$ proportional to the identity (U^{ab}_θ is a constant matrix depending only on one number, the rotation angle; it satisfies $\mathbf{U}_\theta \mathbf{U}^T_\theta = 1$). This freedom to rotate by $\mathbf{U}_\theta$ will be eliminated later by looking at how much information (basically S/N) is carried by each ganglion cell output. We shall insist that no optic nerves are wasted carrying signals with very low S/N.

Returning to the situation with noise, the correlation matrix to be diagonalized here by $K^{ab}(\underline{\mathbf{f}})$ is the one for the signal after filtering by $\mathbf{M}$ (see Fig. 1). To derive $K^{ab}(\underline{\mathbf{f}})$, we go back to the $\mathbf{G} \pm \mathbf{R}$ basis where $M^{ab}(\underline{\mathbf{f}})$ is diagonal in color space. Then we can again apply the single-channel analysis from Atick and Redlich (1992) to each channel separately. This gives two functions $K_\pm(\underline{\mathbf{f}})$ that are chosen to separately whiten the $\mathbf{G} \pm \mathbf{R}$ channels, respectively. Since the complete frequency space correlators in

pendently. More precisely, $H = -\sum_{\{ijk\ldots\}} P_{\{ijk\ldots\}} \log(P_{\{ijk\ldots\}})$, using the complete joint probabilities $P_{\{ijk\ldots\}} \equiv P(O_i, O_j, \ldots)$ for the neural (*e.g.* photoreceptor) outputs O_i with space–time–color index i, while $H_i = -\sum P(O_i) \log[P(O_i)]$. The difference between H and $\sum_i H_i$ measures the amount of statistical dependence of the neural signals on each other: the more dependent, the greater the redundancy, since then more bits effectively carry the same information. Reducing redundancy amounts to finding a transformation on the signals O_i so that after the transformation the ratio $H/\sum_i H_i$ is lowered.

the two channels after filtering by $M_\pm(\underline{f})$ are $M_\pm^2(\underline{f})(R_\pm(\underline{f})+N^2)+N_0^2$, the $K_\pm(\underline{f})$ are therefore

$$K_\pm(\underline{f}) = \frac{\rho^{1/2}}{\left[M_\pm^2(\underline{f})(R_\pm(\underline{f})+N^2)+N_0^2\right]^{1/2}} \tag{2.7}$$

where N_0^2 is the power of the noise that is added following the filter $M^{ab}(\underline{f})$ (see equation 2.2). Equation 2.7 generalizes the whitening filter $K(\underline{f}) = \sqrt{\rho/R(\underline{f})}$ to the case with noise. Now putting equation 2.7 together with equations 2.4 and 2.6, we obtain the complete retinal transfer function — the one measured experimentally —

$$\mathbf{K}_{exp} = \mathbf{U}_\theta \begin{pmatrix} K_+(\underline{f}) & 0 \\ 0 & K_-(\underline{f}) \end{pmatrix} \begin{pmatrix} M_+(\underline{f}) & 0 \\ 0 & M_-(\underline{f}) \end{pmatrix} \begin{pmatrix} 1 & 1 \\ -1 & 1 \end{pmatrix} \tag{2.8}$$

The right-most matrix transforms the **G**, **R** inputs into the $\mathbf{G} \pm \mathbf{R}$ basis. These two channels are then separately filtered by $K_\pm M_\pm$. Finally, the rotation $\mathbf{U}_\theta$, to be specified shortly, determines the mix of these two channels carried by individual retinal ganglion cells.

3 Properties of Solutions

We now use our theoretical solution (equation 2.8) to explain the observed color processing. Specifically, we now show how such diverse processing types as those found in goldfish and primates are both given by equation 2.8 but for different values of the parameter r in the color correlation matrix.

For the case of goldfish, where, as argued in the introduction, one expects only small overlap between R and G (r is small), the two channels in the diagonal basis have eigenvalues $1 \pm r$, which are comparable: $(1-r)/(1+r) \sim 1$. This means that both channels will on average be carrying roughly the same amount of information and will handle signals of comparable S/N. Thus the filters $K_+(\underline{f})M_+(\underline{f})$ and $K_-(\underline{f})M_-(\underline{f})$ are very similar. In fact they are both bandpass filters as shown in Figure 2A for some typical set of parameters. Since these channels are already nearly equalized in S/N, there is no need to rotate them using $\mathbf{U}_\theta$, so that matrix can be set to unity. Therefore, the complete solution (equation 2.8) when acting on the input vectors $\mathbf{R}, \mathbf{G}$, gives two output channels corresponding to two ganglion cell types:

$$\begin{aligned} \mathbf{Z}_1 &= (\mathbf{G}+\mathbf{R})\, K_+M_+ \\ \mathbf{Z}_2 &= (\mathbf{G}-\mathbf{R})\, K_-M_- \end{aligned} \tag{3.1}$$

If we Fourier transform these solutions to get their profiles in space, we arrive at the kernels $K^{ab}(\mathbf{x}-\mathbf{x}')$ shown in Figure 3 for some typical set of

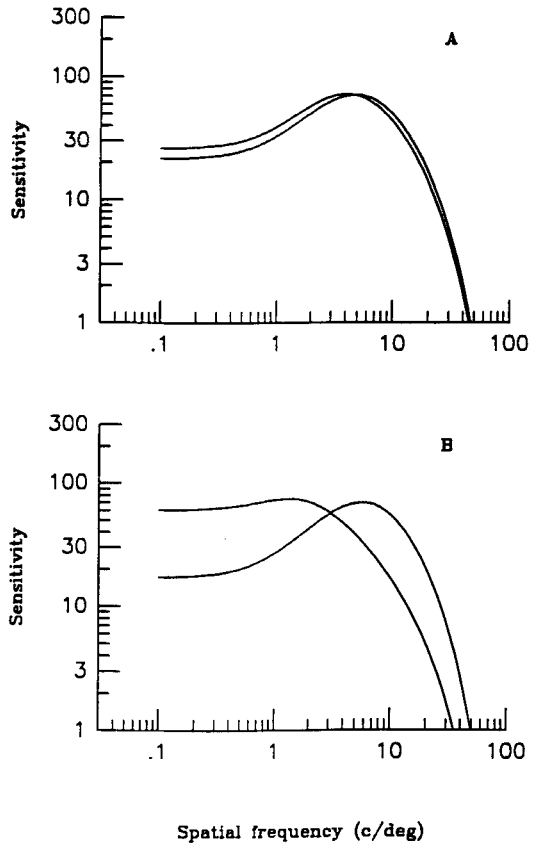

Figure 2: (A,B) The luminance and chromatic channels for the goldfish, *A*, and for primates, *B*. In both figures the curve that is more bandpass-like is the luminance $\mathbf{G}+\mathbf{R}$ channel, while the other is the $\mathbf{G}-\mathbf{R}$ channel. Parameters used are $I_0/N = 5.0$, $\alpha = 1.4$, $f_c = 22.0$ c/deg, $N_0 = 1.0$ for both A and B. The only difference between the A and B is r: for A, $r = 0.2$ while for B, $r = 0.85$.

parameters. The top row is one cell type acting on the **R** and **G** signals, and the bottom row is another cell type. These have the properties of double opponency cells.

Moving to primates, there is one crucial difference which is the expectation that r is closer to 1 since the overlap of the spectral sensitivity curves of the red and green is much greater: the ratio of eigenvalues $(1-r)/(1+r) << 1$. Since the eigenvalues modify the S/N, this means that the $\mathbf{G}-\mathbf{R}$ channel has a low S/N while the $\mathbf{G}+\mathbf{R}$ has much higher S/N. Therefore, $K_-(\underline{f})M_-(\underline{f})$ is a lowpass filter while $K_+(\underline{f})M_+(\underline{f})$ is bandpass as shown in Figure 2B. These two channels can be identified with the chro-

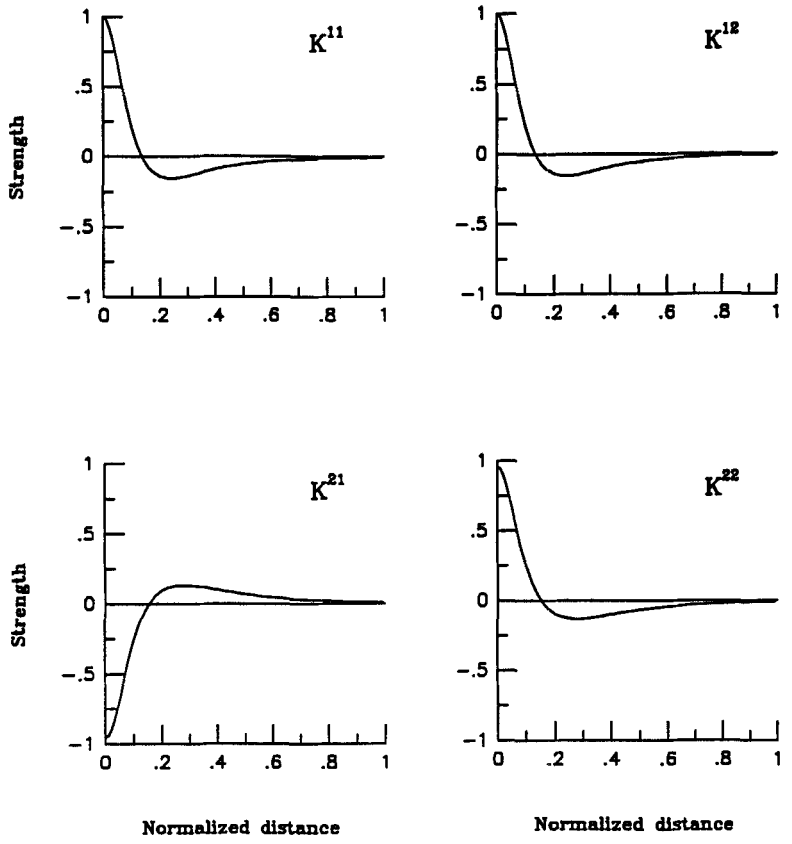

Figure 3: The retinal kernel K^{ab} in the **R** and **G** basis predicted by the theory for $r = 0.2$ (goldfish regime) and for the same parameters used in Figure 2. The top and bottom rows correspond to two different types of retinal ganglion cells predicted by the theory. These cells can be termed double opponent and they are similar to many goldfish ganglion cells.

matic and luminance channels measured in psychophysical experiments, respectively. The curves shown in Figure 2B do qualitatively match the results of psychophysical contrast sensitivity experiments (Mullen 1985): namely the lowpass and bandpass properties of the chromatic and luminance curves, respectively. So according to our theory, these differences in spatial processing come from the hierarchy between the color eigenvalues that leads to different spatiotemporal S/N in the two channels.

Although there is psychophysical evidence that color information in primates under normal conditions is physically organized into luminance and chromatic channels in the cortex (Mullen 1985), this is not how the primate retina transmits the information down the optic nerve (Derrington *et al.* 1984). One reason that might explain why the primate retina chooses not to use the $\mathbf{G}\pm\mathbf{R}$ basis is that the representation of information in chromatic and luminance channels has one undesirable consequence: If we compute the signal-to-noise ratio as a function of frequency in the chromatic channel, given by $(S/N)^2_- = K^2_- M^2_- R_- / \left[K^2_- (M^2_- N^2 + 1)\right]$, and compare it with the corresponding ratio in the luminance channel we find that the ratio $(S/N)_-/(S/N)_+ \ll 1$ because $(1-r)/(1+r) \ll 1$. So for primates, transmitting the information in the luminance and chromatic basis would result in one channel with very low S/N, or equivalently one channel that does not carry much information. Transmitting information at low S/N down the optic nerve could be dangerous, especially since the optic nerve introduces intrinsic noise of its own; it also may be wasteful of optic nerve hardware. What we propose here is to use the remaining symmetry of multiplication by the rotation matrix $\mathbf{U}_\theta$, to "multiplex" the two channels so they carry the same amount of information, that is, such that they have the same S/N at each frequency.

We should point out that the same could have been done for the goldfish but there the two channels (equation 3.1) $(\mathbf{G}+\mathbf{R})K_+(\underline{f})M_+(\underline{f})$ and $(\mathbf{G}-\mathbf{R})K_-(\underline{f})M_-(\underline{f})$ already have approximately equal S/N so the degree of multiplexing is very small or ignorable. In the case of primates, where the hierarchy in S/N between the two channels is large the mixing of the two channels will be significant. In fact the angle of rotation needed is approximately 45°. This leads finally to the following solutions for the two optimally decorrelated channels with equalized S/N ratios

$$\begin{aligned}
\mathbf{Z}_1 &= (\mathbf{G}+\mathbf{R})\,K_+M_+ - (\mathbf{G}-\mathbf{R})K_-M_- \\
&= \mathbf{R}\,(K_+M_+ + K_-M_-) + \mathbf{G}\,(K_+M_+ - K_-M_-) \\
\mathbf{Z}_2 &= (\mathbf{G}+\mathbf{R})\,K_+M_+ + (\mathbf{G}-\mathbf{R})K_-M_- \\
&= \mathbf{R}\,(K_+M_+ - K_-M_-) + \mathbf{G}\,(K_+M_+ + K_-M_-) \qquad (3.2)
\end{aligned}$$

Since for primates, $K_+(\underline{f})M_+(\underline{f})$ and $K_-(\underline{f})M_-(\underline{f})$ are very different, the end result is a dramatic mixing of space and color. For example, cell no. 1 at low frequency has $K_-(\underline{f})M_-(\underline{f}) > K_+(\underline{f})M_+(\underline{f})$ so it performs an opponent $R-G$ processing. As the frequency is increased, however, $K_-(\underline{f})M_-(\underline{f})$ becomes smaller than $K_+(\underline{f})M_+(\underline{f})$ and the cell makes a transition to a smoothing $G+R$ type processing (Derrington *et al.* 1984). In Figure 4, we show the filters in frequency space, in the **R** and **G** basis. These filters are in principle directly measurable in contrast sensitivity experiments. We view the zero crossing at some frequency as a generic prediction of this theory.

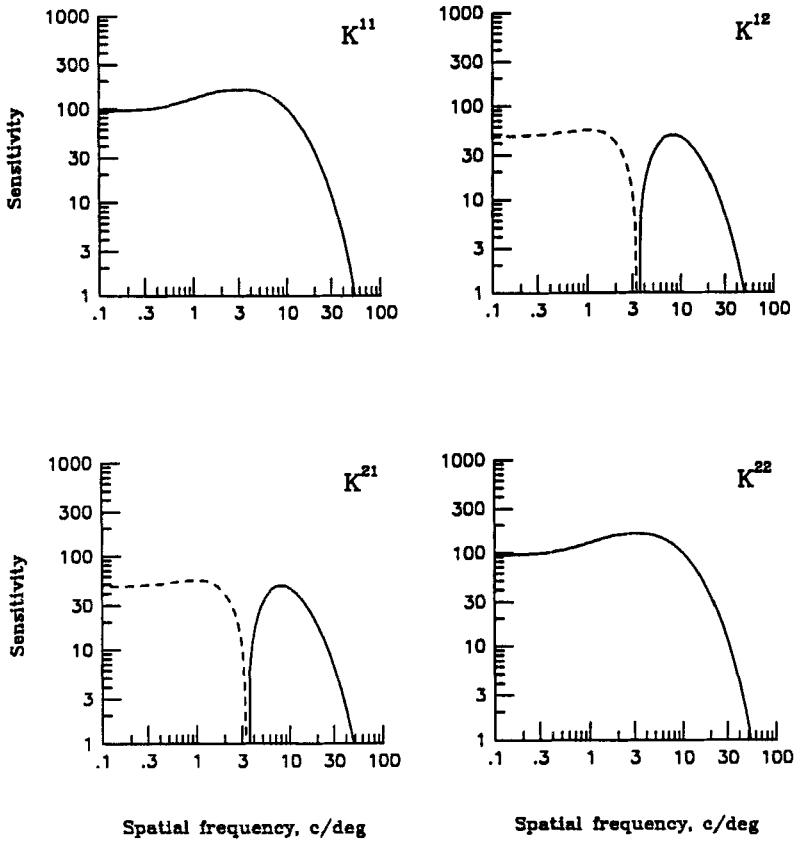

Figure 4: The predicted retinal filter $K^{ab}(\underline{f})$ in the **R** and **G** basis for the parameters in Figure 2 with $r = 0.85$ (primate regime). The solid (dashed) lines represent excitatory (inhibitory) responses. Notice that both cells $\mathbf{Z}_1$ and $\mathbf{Z}_2$ make a transition at some frequency from opponent color coding ($\mathbf{G} - \mathbf{R}$ or $\mathbf{R} - \mathbf{G}$) to nonopponent ($\mathbf{G} + \mathbf{R}$).

In Figure 5 (dashed line), we show how the solutions look for a typical set of parameters after Fourier transforming back to space. We can see cell type 1 summates red mostly from its center and an opponent green mostly from its surround, while for type 2 the red and green are reversed. These cells can be termed single opponency cells, as seen in primates (Derrington *et al.* 1984). One might object that the segregation of the red and green in the center is not very dramatic. Actually, this is due to the

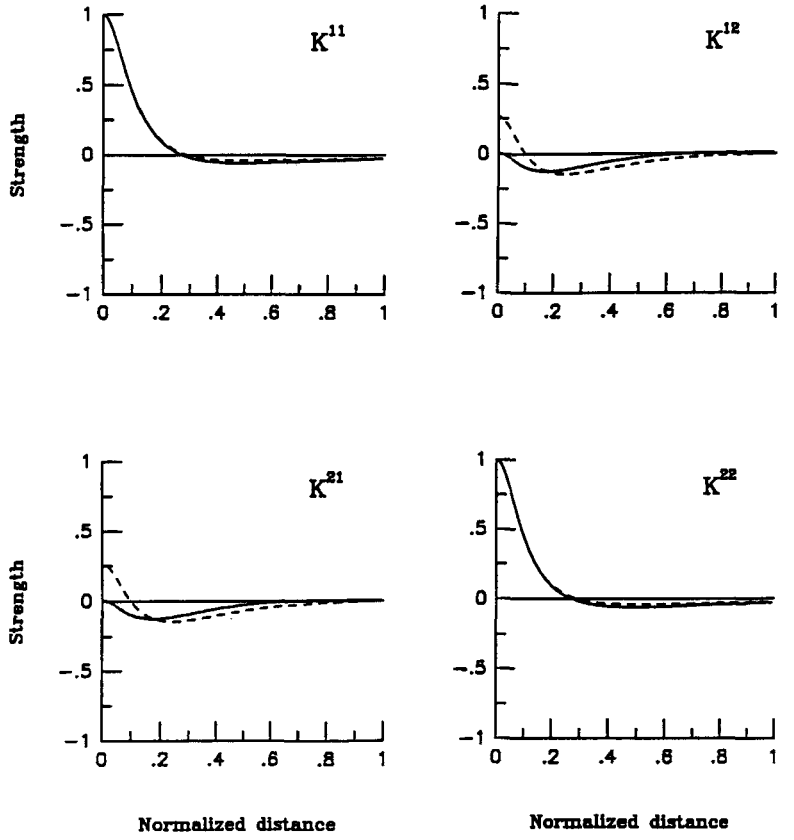

Figure 5: The retinal kernel K^{ab} in the **R** and **G** basis predicted by the theory for $r = 0.85$ (primate regime) and for the same parameters used in the Figure 2 (dashed curves). The solid curves use the same parameters with one exception: the parameter N_0 was allowed to be different in the luminance and chromatic channels by a factor of two. This was done to illustrate that complete color segregation in the cell's center can be easily achieved.

simplified model we have taken. Complete segregation can be achieved if one allows the synaptic noise parameter N_0, which was set to 1 for the dashed line, to be different for the two channels. In fact a difference of 1/2 between the two noises produces the solutions shown by the solid curves in Figure 5.

Acknowledgments

We wish to thank K. Miller for useful comments on the manuscript. Work supported in part by a grant from the Seaver Institute.

References

Atick, J. J., and Redlich, A. N. 1990. Towards a theory of early visual processing. *Neural Comp.* **2**, 308–320.

Atick, J. J., and Redlich, A. N. 1992. What does the retina know about natural scenes? *Neural Comp.* **4**, 196–210; also Quantitative tests of a theory of retinal processing: Contrast sensitivity curves. Preprint no. IASSNS-HEP-90/51.

Atick, J. J., Li, Z., and Redlich, A. N. 1990. Color coding and its interaction with spatiotemporal processing in the retina. Preprint no. IASSNS-HEP-90/75.

Attneave, F. 1954. Some informational aspects of visual perception. *Psychol. Rev.* **61**, 183–193.

Barlow, H. B. 1961. Possible principles underlying the transformation of sensory messages. In *Sensory Communication*, W. A. Rosenblith, ed. MIT Press, Cambridge, MA.

Buchsbaum, G., and Gottschalk, A. 1983. Trichromacy, opponent colours coding and optimum colour information transmission in the retina. *Proc. R. Soc. London Ser. B* **220**, 89–113.

Campbell, F. W., and Gubisch, R. W. 1966. Optical quality of the human eye. *J. Physiol.* **186**, 558–578.

Daw, N. W. 1968. Colour-coded ganglion cells in the goldfish retina: Extension of their receptive fields by means of new stimuli. *J. Physiol.* **197**, 567–592.

Derrington, A. M., Krauskopf, J., and Lennie, P. 1984. Chromatic mechanisms in lateral geniculate nucleus of macaque. *J. Physiol.* **357**, 241–265.

Field, D. J. 1987. Relations between the statistics of natural images and the response properties of cortical cells. *J. Opt. Soc. Am. A* **4**, 2379–2394.

Lythgoe, J. N. 1979. *The Ecology of Vision*. Oxford University Press, Oxford.

Mullen, K. T. 1985. The contrast sensitivity of human colour vision to red-green and blue-yellow chromatic gratings. *J. Physiol.* **359**, 381–400.

Received 8 January 1991; accepted 3 January 1992.